

# The Epidemics of Corruption

Ph. Blanchard\*      A. Krueger †

T. Krueger ‡

University of Bielefeld, Faculty of Physics and BiBoS

P.Martin §

FU-Berlin, Department of Law

## Abstract

We study corruption as a generalized epidemic process on the graph of social relationships. The main difference to classical epidemic processes is the strong nonlinear dependence of the transmission probability on the local density of corruption and the mean field influence of the overall corruption in the society. Network clustering and the degree-degree correlation play an essential role in corruption dynamics. We discuss phase transitions, the influence of the graph structure and the implications for epidemic control. Structural and dynamical arguments are given why strongly hierarchically organized societies like systems with dictatorial tendency are more vulnerable to corruption than democracies. A similar type of modelling can be applied to other social contagion spreading processes like opinion formation, doping usage, social disorders or innovation dynamics.

## 1 Introduction

Corruption seems to be an unavoidable part of human social interaction, prevalent in every society at any time since the very beginning of human history till today. In sharp contrast to the high prevalence of corruption in many

---

\*blanchard@physik.uni-bielefeld.de

†networks@andreakrueger.de

‡tkrueger@physik.uni-bielefeld.de

§peter.martin@schulz-berlin.de

countries and the rather large literature on political, social and economical aspects of corruption there is only a small number of attempts to model the dynamics of corruption in a mathematically quantified way. The modelling approach in these few attempts essentially follows two paths. The first is in the sense of microeconomics and incorporates game theoretic aspects (for a recent model in this direction see the book by Steinrücken [17] and the references therein) or rules for maximizing a certain economically based profit functional ([16][10]). Then a set of differential equations for the evolution of the mean corruption is derived and a stability analysis done on that basis. In these models one usually makes rather detailed assumptions about the underlying organization structure on which the individuals interact. The second line of approach is more in the sense of cellular automata (CA) models with rather simple state variables and local interaction dynamics. For example in the article by Wirl [19] a simple 1-dimensional deterministic cellular lattice automata model is used to describe the propagation of corruption. Nevertheless, as is well known in CA-modelling, the global dynamical picture can be highly complex and nontrivial.

Up to now all these attempts did not take into account the complex network of social relationships as the underlying structure for the spread of corruption. In this article we will present a model for the spread of corruption on complex networks in the spirit of epidemiology. The model describes aspects of the evolution of corruption in a virtual population and incorporates some basic universal features of corruption. The local interaction dynamics of the model is similar to cellular automata but "lives" not on a lattice type graph like most of the CA-models but on complex networks.

Considering corruption as a nonstandard epidemic process relies on the plausible assumption that corruption rarely emerges out of nothing but is usually related to some already corrupt environment which may "infect" susceptibles. Of course the spontaneous decision of somebody to act corruptly is possible and could easily be handled in the model as an external weak source of infection. One of the very special features in corruption propagation which differs from what is used in describing classical epidemic processes is the threshold like dependence of the local transition probabilities. By this we mean that a noncorrupt individual gets infected with high probability if the number of corrupt individuals in the group of his direct social contacts (encoded as the set of neighbors in a "friendship" or acquaintance graph) exceeds a certain threshold number. Otherwise if the number of corrupt individuals in somebodys social neighborhood is below that threshold value there is only

a small probability to get corrupt via such "local" interactions. The second main difference to classical epidemic processes is the mean field dependence of the corruption process. By this we mean that an individual can get corrupt just because there is a high prevalence (or believed prevalence) in the society even when there is no corruption in the local neighborhood. There is another interesting mean field term entering the game, namely the society strikes back to corruption with an efficiency proportional to the fraction of the noncorrupt people. Both mean field terms are nonlinear and together with the local propagation mechanisms they give rise to a rather complex dynamical picture.

## 2 What is corruption?

Corruption is a substructure of human social interaction. Common sense associates corruption mainly with a deviation from fair play interaction in the development of social relations. Clearly what is meant by fair play depends on the cultural context of a given population/society. This vague description of corruption is in the spirit of sociology and psychology and differs from the more narrow corruption concepts usually considered in economics or political sciences. There, corruption is mainly seen as a misuse of public power to gain profit in a more or less illegal way. In any case, corruption has many different faces in its concrete appearance and no single model approach will be able to describe the whole picture in an adequate way. But this does not at all imply that mathematical models are useless in this situation. They can provide a substantial improvement in our understanding of corruption as long as one clearly defines the aim and limitations of the taken approach.

For the model approach developed in this article we will use the notion of corruption in the more general, first sense. More precisely our intention is to describe changes in mind ranging from damming of corruption as a criminal act to accepting corruption as an attractive option. Therefore in this paper we do not introduce the group of state representatives or officials since we assume that the essential changes in mind which allow corrupt acts happen long before an individual is in the position to act corruptly. Empirical investigations about motives and "typology" of corrupt actors (see [3] for results from case studies in Germany) have shown that the majority of individuals involved in corruption affairs are highly educated, well positioned with respect to social status and do not think to have done something wrong,

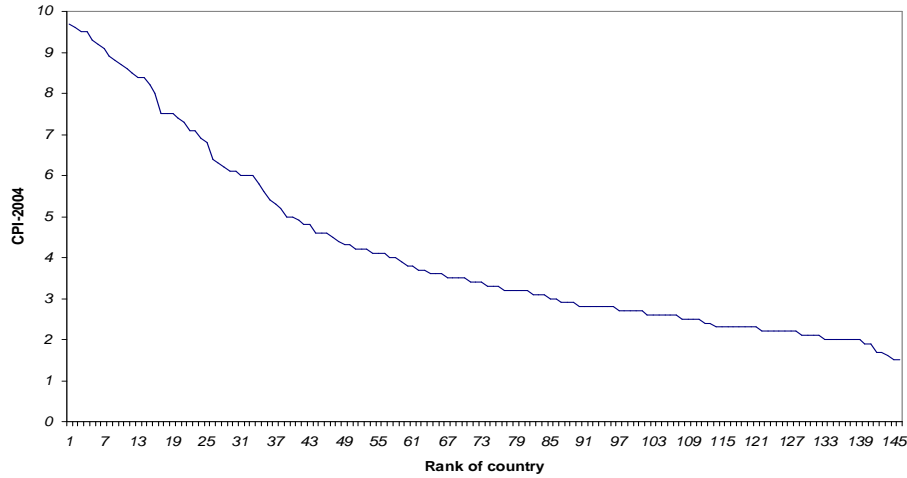


Figure 1: Corruption Perception index 2004 versus rank

indicating the importance of mind changes prior to corrupt acts.

There is a notorious problem in finding good empirical data which would allow to estimate the prevalence of corruption. Probably the greatest effort over the last years to measure the degree of corruption in various countries was made by "Transparency International" (TA), a non profit group of individuals and organizations which are highly concerned by the lack of sound data. Since 1995 they publish a yearly corruption report and a so called Corruption Perception Index (CPI) [18]. TA is well aware of the subjectivity in peoples perception of corruption but hopes that the large number of cases involved in the CPI averages out most of the bias. Figure 1 gives a CPI-rank plot of the 2004 date from TA. Note that a value of 10 for the CPI corresponds to the absence of corruption. For 2004 Finland holds the top ranking and Germany is on place 15 with an index of 8.2.

It is not our aim to explain the values of the CPI or other corruption data sets, since this would require a semirealistic modelling of the social and economical structure of individual countries which is completely illusionary at the present stage of research. Rather we want to demonstrate which scenarios are dynamically possible and whether there are phase transitions.

### 3 Corruption as a generalized epidemic process

In this section we first describe the basic setting for our model structure. Refinements and more detailed aspects will be discussed later on. Due to the common view, corruption is first of all a property of the relations between individuals irrespectively which definition of corruption one uses. Since an act of corruption requires that at least one of the participants in a corrupt relation has a mental state which tolerates or even assigns a positive value to (his personal view of) corruption we will focus mainly on the spread of this mental state change (from not accepting to accepting corrupt acts as an option for one's own activities). Therefore to discuss corruption as an epidemic process in the afore mentioned sense it is useful to assign a corruption property to the individuals themselves. In the simplest case we just have a time dependent 0 – 1 state variable  $\omega(x, t)$  assigned to each individual, encoding whether the vertex is corrupt (1) or not (0) at time  $t$  (of course more refined scales for the degree of corruption are possible and will be discussed in a forthcoming paper). The underlying structure on which corruption spreads is a given finite graph  $G$  from a random graph space  $\mathcal{G}$  with fixed vertex set  $V = \{1, \dots, n\}$ . Furthermore we consider in this article only stationary graphs with no changes in time on the underlying graph structure (the study of corruption on evolutionary graphs requires a paper in its own). The dynamics is specified by conditional transition probabilities ( $p_{ij}(x)$ ) which depend mainly on the states on  $B_1(x) = \{y : d(x, y) \leq 1\}$  and a meanfield term reflecting the influence of the total prevalence of corruption in the society. Here  $d(., .)$  is the usual graph metric on  $G \in \mathcal{G}$  and  $d(x)$  is the degree of  $x$ . We define  $b_t := \frac{1}{N} \sum_{y \in V} \omega(y, t)$  as the density of corruption at time  $t$ . The standing assumptions on ( $p_{ij}(x)$ ) are the following:

$$\begin{aligned}
 p_{01}(x) &= \Pr \{ \omega(x, t+1) = 1 \mid \omega(x, t) = 0 \} = f_x \left( \sum_{y \sim x} \omega(y, t) \right) + \beta(x) \cdot b_t^2 \\
 p_{10}(x) &= \Pr \{ \omega(x, t+1) = 0 \mid \omega(x, t) = 1 \} = \gamma(x) \cdot [1 - b_t]
 \end{aligned} \tag{1}$$

in other words the probability to become corrupt depends only on the local prevalence of corruption among the neighbors and the mean corruption in the society and individuals who became corrupt can cure from corruption with a rate proportional to the density of the noncorrupt individuals in the

society. In classical i.i.d. epidemics one would have the following as functional dependence for the local part of the conditional probabilities:  $f(k) = 1 - (1 - \varepsilon)^k$  which is for small  $\varepsilon$  and  $k$  proportional to  $\varepsilon k$ . For corruption the function  $f$  is more like in voter models, that is below a critical value  $\Delta(x)$  of the number of corrupt individuals in  $B_1(x)$  the value of  $f$  is close to zero and above  $\Delta(x)$  it is a number  $\alpha(x)$  much larger than zero. Due to this property local clustering can force the epidemics to spread whereas in classical epidemic processes high clustering slows down the spread of an infection due to reinfection of the already infected. We want to illustrate this by two simple examples.

**Example 1** *The simplest, almost trivial example is the  $\mathbb{Z}^1$  lattice with additional edges to the next-nearest neighbors. Setting  $f(1) = \mu > 0$  and  $f(i) = 1$  for  $i > 1$  it is easy to see that there is a nonzero probability for infecting all vertices starting with one infected individual at time 0.*

**Example 2** *The infection function  $f$  will be the same as in example 1. We start with a regular tree of degree 3. Replacing each vertex by a triangle and gluing the triangles along the former edges of the regular tree gives a regular graph of degree 4 where the triangle corners act now as the new vertices. In each neighbor pair of triangles  $(A, B)$  (that are the triangles which have a common vertex) we form an edge randomly between the set of vertices lying in  $A \setminus B$  and  $B \setminus A$  (see Fig. 1). Once a triangle is infected the corruption jumps to all the three neighbor triangles due to the extra random edge present between each neighbor pairs of triangles. Hence again we have a nonzero probability that the whole graph becomes infected.*

In the above examples we have used a very simple and somehow extreme form of the infection function  $f$ . In the following we will investigate the situation for two canonical subclasses of infection functions. We say that  $f$  is a vertex independent, fixed threshold infection function if there is a  $\Delta$  such that  $f(i) = \varepsilon$  for  $0 < i < \Delta$  and  $f(i) = \alpha \gg \varepsilon$  for  $i \geq \Delta$ . For the second class of functions we assume the threshold to be degree dependent. Namely we call  $f_x$  a vertex dependent, relative threshold function if for some  $\delta \in (0, 1)$  we have  $f_x(i) = \varepsilon$  for  $0 < i < \delta d(x)$  and  $f(i, x) = \alpha \gg \varepsilon$  for  $i \geq \delta d(x)$ . Furthermore we say that  $f$  is a voter-type infection function if  $f(i, x) = \varepsilon$  for  $i < \lfloor \frac{1}{2}d(x) \rfloor$  and  $f(i, x) = \alpha$  for  $i \geq \lfloor \frac{1}{2}d(x) \rfloor$ . In this paper we will mainly investigate the spread of corruption for the fixed threshold case.

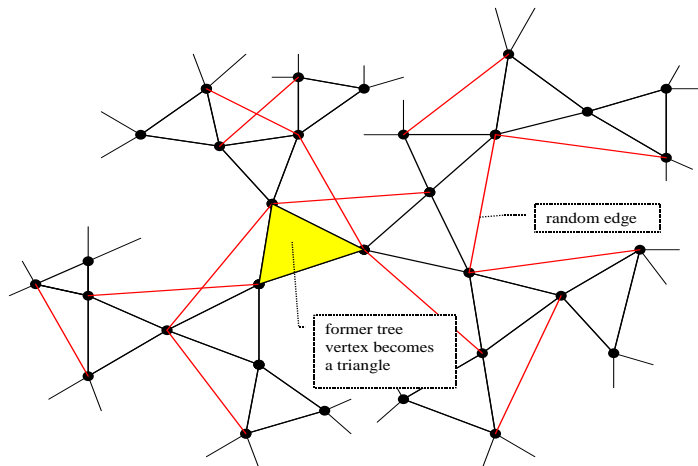


Figure 2: A highly clustered network with underlying tree structure.

<i>process name</i>	<i>characteristic</i>	<i>typical value</i>
$\alpha$ - process	the local transmission process for # of corrupt neighbors $\geq \Delta$	$\alpha \gg \varepsilon, \beta, \gamma$
$\beta$ - process	the mean field transmission process due to the total prevalence or perception of corruption	$\varepsilon < \beta < \gamma$
$\gamma$ - process	the corruption recover/elimination process due to the fight of the society against corruption	$\beta \leq \gamma < \alpha$
$\varepsilon$ - process	the classical local epidemic process for # of corrupt neighbors $< \Delta$	$\varepsilon \ll \alpha, \beta, \gamma$

Table 1: the different processes for the corruption dynamics

To distinguish between the different ways in which an individual can become corrupt we will speak about the  $\alpha, \beta, \varepsilon$  or  $\gamma$ - process. For convenience of the reader we give in tabular 1 a summary of the different processes.

Note that in contrast to standard voter models we do not have the possibility of a locally induced backflip from the corrupt state to the noncorrupt. A kind of quenched disorder could easily be introduced by randomizing the relevant parameters individually but this will be the subject of a forthcoming paper. Generalizations of classical epidemic dynamics to processes with a local threshold have recently also been studied in the context of models of contagion (see [9] and references therein) but not yet been mixed with global

mean field processes.

## 4 The structure of social networks

In the last 10 years there has been an enormous progress in understanding the fine structure of social networks. This is mostly due to the availability of large data sets for some special social networks like E-mail correspondence, coauthorship network in scientific publications and movie actor networks to name just a few prominent examples. All these networks of social relations share three remarkable properties of the associated graph which are: 1) the diameter scales at most logarithmically in size 2) the graphs have a very high, asymptotically non-vanishing clustering coefficient- in other words the graphs are locally far from being tree-like 3) the degree distribution follows a power law (scale-free graphs). Properties 2 and 3 have striking consequences for the spread of corruption as will be discussed later on.

There exists meanwhile a large collection of algorithms to generate complex networks with the above mentioned properties.

A widely used quantity to measure the local clustering is the triangle number  $A(x) := \#\{\text{triangles containing } x\}$  and it's averaged value  $\bar{A}$ . A natural generalization is the  $k$ - clique number  $C_k(x)$  defined as the number of complete graphs of order  $k$  containing  $x$ . In social network graphs  $A(x)$  is usually proportional to  $d(x)$  and  $\bar{A}$  becomes independent of the population size for large  $N$  and stays bounded away from zero. Another very remarkable property of real networks is the power-law distribution for the degree. By an asymptotic power-law distribution for a discrete random variable  $d$  we denote every functional behavior of the form  $\Pr\{d = k\} = k^{-\lambda+o_k(1)}$  with exponent  $\lambda > 1$ . Most real networks have exponents between 2 and 4 (see [1] for an excellent overview). Classical epidemic processes on such graphs have been studied by many authors, and perhaps the most astonishing result in this context is the absence of an epidemic threshold in case the exponent is below 3 ([15]). This phenomenon is related to the existence of a massive center of size independent diameter induced by the high number of hubs (vertices with an exceptional large degree). Hubs play also a significant role for  $\alpha$  - process as will be explained in the next section.

One of the main differences between corruption epidemics and classical epidemics is the different effect of clustering on the epidemic threshold and the total number of infected individuals. In the classical situation any

epidemics will be slowed down by the presence of local cycles due to the high probability of reinfection. In corruption epidemics local clustering may speed up the propagation of corruption due to the nonlinear dependence of the infection probability on the number of infected neighbors as was already demonstrated in example 1 in the previous section. In the next section we will give two further examples where the strength of this effect can explicitly be computed.

## 5 Phase transitions for the $\alpha$ - process

In this section we want to look at some threshold properties associated to the  $\alpha$ - process. We are still far from a good understanding of the quantitative picture of this kind of processes for a given type of graph, which is mainly a consequence of our lack of knowledge how to handle graphs with high local clustering in a mathematical satisfactory way. In this section we want to state just some general observations and numerical results concerning the spread of threshold-like dynamics. Furthermore we will analyze two examples of tree-like graphs which might serve as an illustration. A more careful mathematical analysis of  $\alpha$ - processes requires a paper in its own.

One of the remarkable differences between a classical epidemic process and a process based on local threshold dynamics is the dependence on the initial number of "infected" vertices in the latter case. Classical epidemics does not know such things- either an epidemic process is overcritical (reproduction number  $R_0 > 1$ ) and a single initial infected vertex infects with with positive probability a positive fraction of the whole population, or the process is below criticality ( $R_0 < 1$ ) and all infected will die out respectively become healthy. In corruption epidemics both parts - the mean field process as well the local  $\alpha$ - process - can have phase transitions with respect to the initial number of corrupt vertices. That means, there is critical initial density of corrupt vertices  $b_0^c$  such that for initial densities below  $b_0^c$  the number of infected stays as it is or goes down to zero. Above  $b_0^c$  the entire population becomes corrupt with high probability. As an illustration we give in Fig. 3 the dependence of  $b_0^c$  on the edge density  $\frac{M}{N}$  on a classical random graph space  $\mathcal{G}(N, M)$  with  $N$  vertices and  $M$  edges.

Although in this paper we mainly concentrate on the case of absolute threshold values  $\Delta$  we give for comparison in Fig.4 the edge density dependence result for a relative, degree dependent threshold  $\Delta(x) = \lceil 0.8 \cdot d(x) \rceil$ .

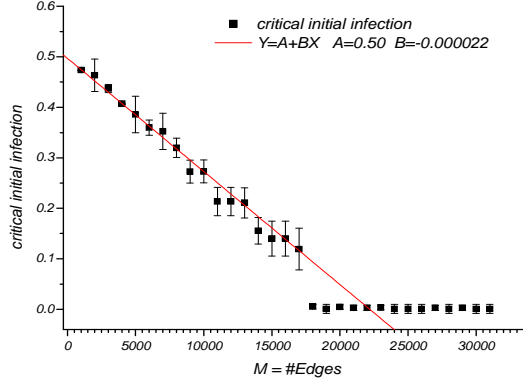


Figure 3: numerical estimation of the critical initial density  $b_0^c$  as a function of the number of edges  $M$  for the following parameter values:  $\Delta = 5$ ;  $\alpha = 0.35$ ;  $\beta = 0.08$ ;  $\gamma = 0.04$ ;  $\varepsilon = 0.005N = 4000$ . Vertical segments are errorbars over 20 runs.

There is still a critical density but its value increases with the edge density since the mean threshold increases now proportional to the mean degree. As already mentioned in section 3 one expects that the presence of clustering (respectively many triangles) decreases the critical density  $b_0^c$  since the  $\alpha$ -process can propagate more easily. In Fig. 5 the effect of the increase of the triangle number is clearly to see. Here we used a modified  $\mathcal{G}(N, M)$  random graph space where randomly triangles are added (keeping the total number of edges constant). The threshold value  $\Delta$  was chosen to be 2 since for higher  $\Delta$  one has to add higher order complete subgraphs instead of triangles.

The next figure (Fig. 6) shows the dependence of the critical density on  $\Delta$ . The two curves represent the threshold values for an end-prevalence of 10 respectively 90 percent. Since the mean degree in this simulation is about 6.5 one has a vanishing contribution of the  $\alpha$ - process above  $\Delta = 8$ . The critical threshold  $b_0^c$  stays than essentially at a value given by the mean field process (see next section for details). To get an impression of the contribution of the different kind of processes (local  $\alpha$  and  $\varepsilon$ , global  $\beta$  and  $\gamma$  - for details see next section) to the end-prevalence we give in Fig. 7 the accumulated number of state changes caused by each of the subprocesses till saturation. For small values of  $\Delta$  the  $\alpha$ - process dominates all others.

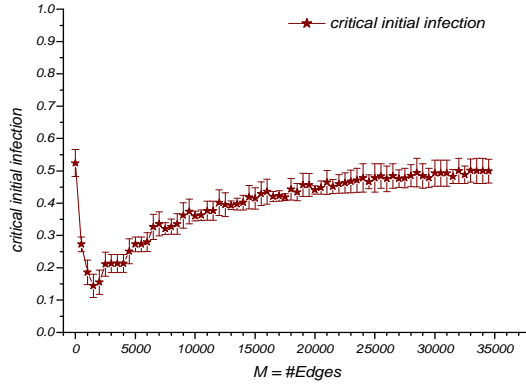


Figure 4: critical initial density  $b_0^c$  as a function of the number of edges  $M$  for relative delta and parameter values:  $\Delta(x) = \lceil 0.8 \cdot d(x) \rceil$ ;  $\alpha = 0.35$ ;  $\beta = 0.08$ ;  $\gamma = 0.04$ ;  $\varepsilon = 0$ ;  $N = 4000$ . Vertical segments are errorbars over 20 runs.

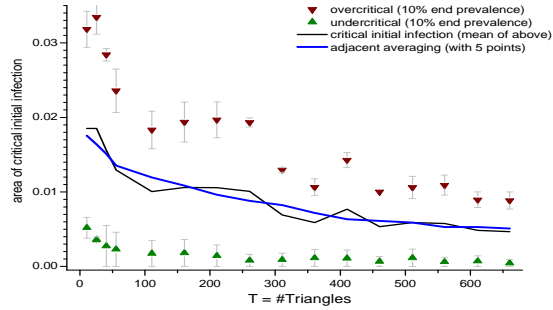


Figure 5: Critical density  $b_0^c$  versus triangle density for the parameter values:  $\Delta = 2$ ;  $\alpha = 0.3$ ;  $\beta = 0.08$ ;  $\gamma = 0.04$ ;  $\varepsilon = 0.005$ ;  $N = 1000$ ;  $M = 2000$ .

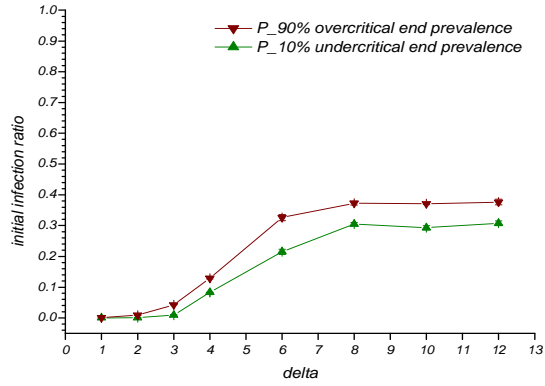


Figure 6: Lower and upper bounds for the critical density  $b_0^c$  as a function of  $\Delta$  for the following parameter values:  $N = 1500$ ;  $M = 5000$ ;  $\alpha = 0.35$ ;  $\beta = 0.08$ ;  $\gamma = 0.04$ ;  $\varepsilon = 0.005$

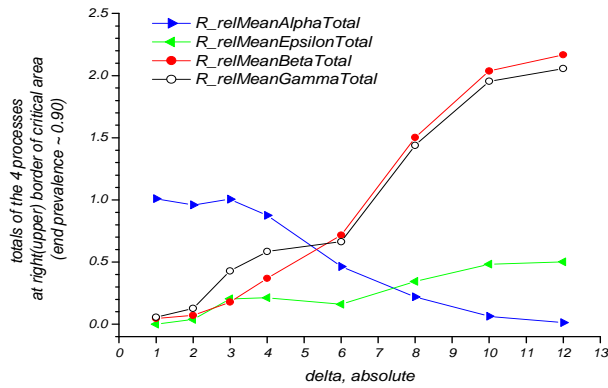


Figure 7: Total number of state changes splitted according to the different subprocesses as a function of  $\Delta$  for the same parameter values as in Fig.6.

We turn now to a more theoretical consideration, namely which type of vertices (type in the sense of degree and local clustering) are especially well suited for the propagation of corruption via the  $\alpha$ -process. Assume we have given a random scale free graph space  $\mathcal{G}$  with  $N$  vertices. We further assume that there are two types of edges (according to the way they were generated) the independent ones, generated at random with just preferences to the degree (like the preferential attachment rule by Albert&Barabasi or the "Cameo-Principle" in [4]) and local ones which are relevant for the creation of triangles. Let further the (asymptotic) degree distribution given by  $\varphi(k) := \Pr\{d(x) = k\} = \frac{B(k_0)}{k^\lambda}$  with  $k_{\min} \geq k_0$  and  $B(k_0)$  the normalization constant. The independent edges are generated with probability  $p_0$  and each individual generates  $k_0 > 2$  edges by himself. From [4] one knows that the triangle number  $A(x)$  is proportional to  $d(x)$  with a proportionality constant  $C(p_0)$ . A basic quantity in highly clustered networks is the probability  $q(x)$  that two random chosen elements from  $N_1(x | d(x) > 1)$  have a common edge. Since  $A(x) \sim c_T d(x)$  one obtains for the conditional probability  $q_k(x) := \Pr\{z \sim y | z, y \in N_1(x) \wedge d(x) = k\} \sim \frac{2c_T}{k-1} \sim \frac{2c_T}{k}$ . Assuming that the generation of triangles is a sufficiently independent process one obtains for the conditional  $l$ -clique number  $\mathbb{E}(C_l(x) | d(x) = k) = \binom{k}{l-1} \left(\frac{2c_T}{k}\right)^{\frac{(l-1)(l-2)}{2}} \sim \frac{k^{(l-1)(1-\frac{l-2}{2})}}{(l-1)!} \cdot \text{const.}$  Here  $C_l(x)$  is the number of  $l$ -cliques (complete graphs of order  $l$ ) containing  $x$ . For  $l > 4$  the power in the  $k$ -dependence gets negative and hence the high degree vertices contribute almost nothing to the Clique-clustering. Of course all this consideration rely on the assumption of some kind of independence in the triangle-formation process. In any case this results indicate that highly clustered medium degree vertices are especially well suited for the spread of corruption. A similar kind of analysis can be carried out for random graph models which have an intrinsic high probability to generate local cliques e.g. intersection graphs (for an introduction to random intersection graphs and comparison with Erdős-Renyi random graphs see [12] and [11]). The above arguments seem to support the conjecture that in corruption epidemics the vertices from the tail of the degree distribution play a less dominant role. This is indeed true in the case of a relative, degree-dependent threshold where hubs are much more difficult to infect than medium or low degree vertices. For absolute thresholds in the  $\alpha$ -process the situation is more complex since for scale free degree distributions with small exponents ( $\lambda < 3$ ) there are other mechanisms than local clustering which can cause a radical dropdown of the critical initial density. In

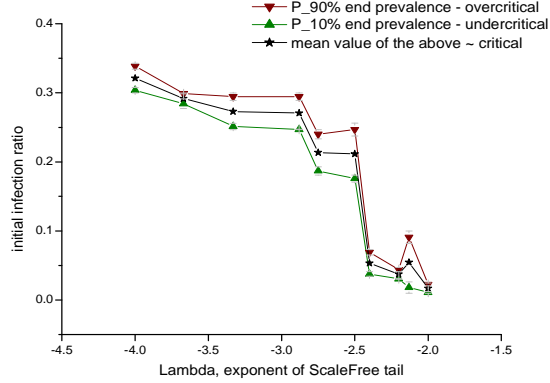


Figure 8:  $b_0^c$  as a function of the exponent  $\lambda$  in a scale-free degree distribution with parameters:  $N = 20000$ ;  $M = 50000$ ;  $\Delta = 5$ ;  $\alpha = 0.35$ ;  $\beta = 0.08$ ;  $\gamma = 0.04$ ;  $\varepsilon = 0$

Fig.8 and Fig.9 we give numerical results for the relation between the critical density  $b_0^c$  and the exponent  $\lambda$  keeping the edge density fixed. There is a clear phase transition around  $\lambda \sim 2.3$  for  $\Delta = 5$  and  $\lambda \sim 2.9$  for  $\Delta = 2$ . The explanation of this observation is closely related to a structural phase transition in scale free random graphs at  $\lambda = 3$  - namely that for most vertices  $x$  an asymptotically positive fraction of all vertices has bounded distance to  $x$ . To link this property with the  $\alpha$  - process one has to look more closely on the degree-degree correlation in scale-free graphs. Depending on the choice of the model one can have very different correlations like:

$$\Pr \{x \sim y \mid d(x) = k \wedge d(y) = k'\} \simeq \text{const} \cdot \frac{k + k'}{N} \text{ or} \quad (2)$$

$$\Pr \{x \sim y \mid d(x) = k \wedge d(y) = k'\} \simeq \text{const} \cdot \frac{k \cdot k'}{N} \quad (3)$$

. Formula 2 holds for instance for the Cameo - model ([4]) whereas formula 3 is valid for scale-free graphs generated via the Molloy&Reed algorithm (the later one represents the random graph space containing all graphs with a given scale-free degree distribution equipped with the uniform measure and was used for the simulations in Fig.8 and 9). Evolutionary graphs like the Albert&Barabasi model have usually asymmetric and more complicated

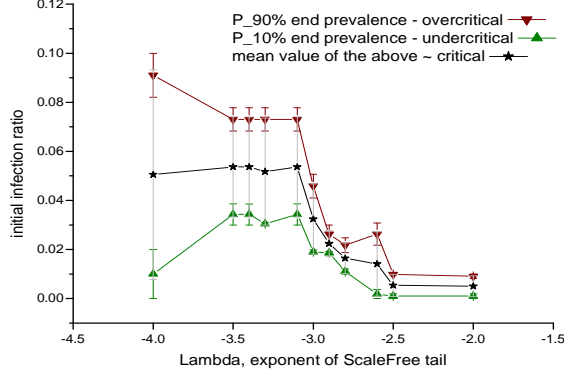


Figure 9: upper and lower bounds for  $b_0^c$  as a function of the exponent  $\lambda$  in a scale-free degree distribution with parameters:  $N = 20000$ ;  $M = 30000$ ;  $\Delta = 2$ ;  $\alpha = 0.35$ ;  $\beta = 0.08$ ;  $\gamma = 0.04$ ;  $\varepsilon = 0$

correlations. Since a detailed analysis of the  $\alpha$  - process for scale-free graphs is beyond the scope of this paper we just give a heuristic outline why in graphs with a correlation as in formula 3 the threshold density  $b_0^c$  tends to zero as  $N \rightarrow \infty$  for exponents  $\lambda < 3$ . For fixed  $b_0 > N^{\frac{1}{\lambda} - \nu}$  and  $\nu > 0$  (note that the typical maximal degree is about  $N^{\frac{1}{\lambda}}$ ) it is obvious that vertices  $x$  with  $d(x) \geq k_0 \gg \frac{\Delta}{b_0}$  get almost surely infected (as  $N \rightarrow \infty$ ) via the  $\alpha$  - process as soon as  $\gamma < \alpha$ . Let  $A_{k_0}$  be the set of such vertices. On the other side it follows from 3 that a vertex  $y$  with  $d(y) = k < k_0$  is linked to the set  $A_{k_0}$  with probability

$$q_k \sim 1 - \prod_{k' \geq k_0}^{k_{\max} \sim N^{\frac{1}{\lambda}}} \left( 1 - \frac{\text{const} \cdot k \cdot k'}{N} \right)^{\text{const} \cdot \frac{N}{(k')^\lambda}} \quad (4)$$

$$\sim 1 - e^{-\text{const} \cdot \frac{k}{N} \sum_{k' \geq k_0} N \cdot \frac{k'}{(k')^\lambda}} \sim 1 - e^{-\text{const} \cdot k \frac{1}{k_0^{\lambda-2}}} \quad (5)$$

. Since  $q_k$  is close to 1 for  $k > k_0^{\lambda-2}$  one has an almost sure multiple linkage of vertices  $y$  with  $d(y) > k_0^{\lambda-2} < k_0$  to the set  $A_{k_0}$ . These vertices get now again infected via the  $\alpha$  - process. By iterating this procedure one may arrive at an positive  $N$ - independent infection density  $b_t \gg b_0$  such that the  $\beta$  - process is overcritical and finally the whole vertex set becomes

corrupt. The mechanism described requires  $N$  to be large and therefore we conjecture that the difference to the numerical results depicted in Fig.8 (phase transition at  $\lambda < 2.3$  instead of 3) is due to finite size effects. In the case of  $\Delta = 2$  (Fig.9) the finite size effects are smaller and the phase transition is closer to 3. A similar kind of arguments shows, that the expected path-length is finite for  $\lambda < 3$ . Namely since the expected number  $S_l$  of vertices at distance  $l$  from a vertex  $x$  with degree  $k_0$  is approximately given

$$\text{by } (const)^l \cdot \sum_{k_1, \dots, k_l}^{N^{\frac{1}{\lambda}}} \frac{k_0 \cdot k_1 \cdot k_1 \cdot \dots \cdot k_{l-1} \cdot k_{l-1} \cdot k_l}{(k_1)^\lambda \cdot \dots \cdot (k_{l-1})^\lambda} \sim const \cdot k_0 \cdot N^{\frac{(l-1)(3-\lambda)}{\gamma}} \text{ for } \lambda < 3 \text{ (note}$$

that this expression is only valid for  $l$  s.t.  $\frac{(l-1)(3-\lambda)}{\gamma} \cdot \log k_0 < 1$ ). The essential diameter  $diam_e$  (a large fraction if the whole vertex set is within a ball of diameter  $diam_e$ ) is then given by the smallest  $l$  such that  $\frac{(l-1)(3-\lambda)}{\gamma} > 1$  (for a more extensive discussion of the notion of essential diameter see [5]). For  $\lambda = 2$  one obtains therefore  $diam_e = 3$ . For  $\lambda > 3$  the essential diameter is no longer bounded but grows logarithmically in  $N$ . It is interesting that the jump in the critical density at 2.3 in Fig.8 coincides with a jump in diameter from 4 to 5. A small essential diameter can have fatal consequences for corruption epidemics since most vertices are closely linked to hubs and, as was outlined above, hubs are with high probability corrupt. A precise estimation of the dependence of  $b_0^c$  from  $N$ ,  $M$  and  $\lambda$  requires a careful discussion of the involved constants. For scale-free graphs with additive degree correlation like Cameo-graphs one still has a bounded essential diameter for exponents less than 3. But the first argument about chains of almost sure linkages from high degree to low degree vertex sets can not be adopted. One expects therefore a higher value of the critical density  $b_0^c$ . In Fig.10 and Fig. 11 we give numerical results for a scale-free graph with additive degree-correlation generated via a modified Molloy&Reed algorithm <sup>1</sup>

To compare with the multiplicative case we have chosen the same parameters and degree-distribution as for Fig.9. There is a clear increase of  $b_0^c$  to

---

<sup>1</sup>In the usual Molloy&Reed algorithm one generates  $d(x)$  virtual vertices for each vertex  $x$  and makes than a random matching between the virtual vertices. Two vertices  $x$  and  $y$  are connected by an edge if there is an edge between two corresponding virtual vertices. To generate an additive degree correlation we mark  $M$  virtual vertices as red such that each vertex  $x$  has at least one red and at most  $C \lceil \frac{M}{N} \rceil$  red associated virtual vertices (if there are not too many vertices with very small degree, the constant  $C$  can be chosen as  $\lceil \frac{M}{N} \rceil$ ). Than the marked red virtual vertices are randomly matched with the unmarked ones.

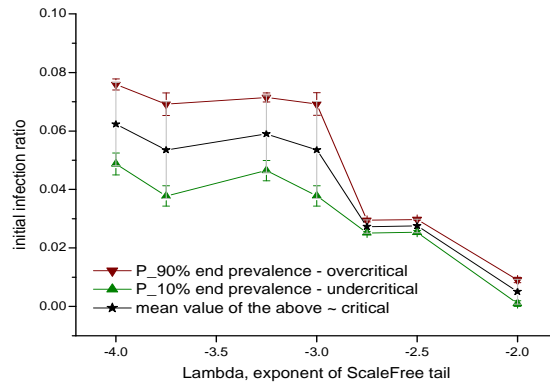


Figure 10: upper and lower bounds for  $b_0^\epsilon$  as a function of the exponent  $\lambda$  in a graph with scale-free degree distribution, additive degree correlation and parameters:  $N = 20000$ ;  $M = 30000$ ;  $\Delta = 2$ ;  $\alpha = 0.35$ ;  $\beta = 0.08$ ;  $\gamma = 0.04$ ;  $\epsilon = 0$

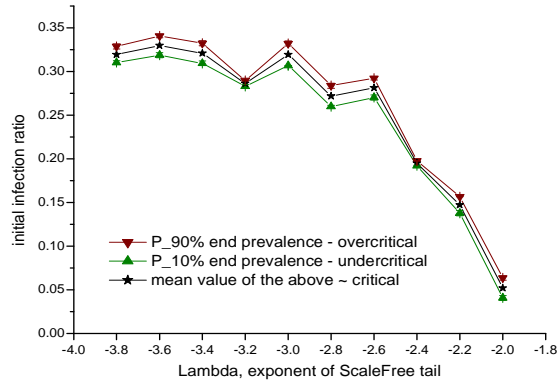


Figure 11:  $b_0^\epsilon$  as a function of the exponent  $\lambda$  in a scale-free degree distribution with parameters:  $N = 20000$ ;  $M = 50000$ ;  $\Delta = 5$ ;  $\alpha = 0.35$ ;  $\beta = 0.08$ ;  $\gamma = 0.04$ ;  $\epsilon = 0$

observe but, although unlikely, it remains open whether there is a vanishing threshold in the limit  $N \rightarrow \infty$ . For intermediate couplings we still expect  $b_0^c(N) \rightarrow 0$  as  $N$  diverges for  $\lambda < \lambda_c \in (2, 3)$  where  $\lambda_c$  depends on the concrete model. It is remarkable that low  $\lambda$  and a tendency to multiplicative correlation is mainly expected to hold in societies with strong hierarchical structures of social dependencies e.g. dictatorships (see [8] for details), whereas democracies are characterized by less strong degree correlation.

Finally we will discuss two examples of graph structures where the critical infection density can be explicitly be computed. The first one is a regular infinite tree of degree 4 where of course no triangles are present (see Fig. 12).

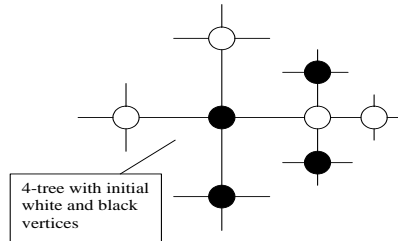


Figure 12: Segment of a regular infinite tree of order 4

. The second structure is a regular infinite graph of again of degree 4 with positive local cluster coefficient ( $A(x) = 2$ ) and a global tree-like structure (see Fig.13).

In both cases an exact computation of the critical infection density is possible. We give a short outline for the case of threshold value  $\Delta = 2$  and  $\alpha = 1$  (the case  $\alpha < 1$  requires more lengthy computations but can be done in a similar fashion) and start with the case of the regular 4 tree. An initial configuration is given by marking each vertex with probability  $p$  as noncorrupt (black) and with probability  $1 - p$  as corrupt (white). We ask for the critical probability  $p_c$  such that for  $p < p_c$  almost surely the entire tree becomes white (corrupt) and for  $p > p_c$  there remains an infinite cluster of noncorrupt (black) vertices with probability one. Note that no finite cluster of black vertices -that is a finite black subgraph surrounded by white vertices- can survive so there are either infinite black clusters or none.

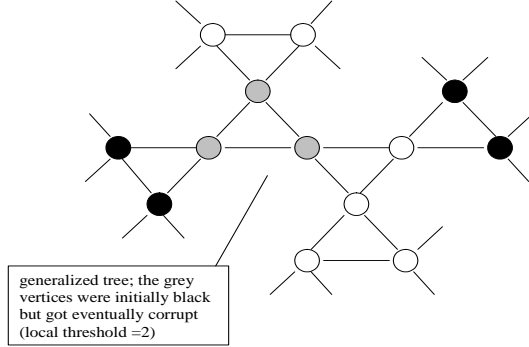


Figure 13: Segment of an infinite generalized tree (degree 4 and branching number 3)

We call an invariant infinite black cluster immune. Since  $\Delta = 2$  any vertex in an immune cluster must have at least three black neighbors from that cluster. Denote by  $T_R(3)$  the rooted tree with outdegree 3 (fixing a root gives a canonical direction to the edges of the tree so it makes sense to speak about the outdegree of a vertex). Every vertex has degree 4 except the root which has degree 3. Let  $x$  be the  $p$ -dependent probability that the root is contained in an immune cluster (as a subgraph of  $T_R(3)$ ) conditioned that the root vertex is initially black. By arguments from the general theory of branching processes  $x$  equals the largest solution of the following recursion equation

$$x = \underbrace{p^3 x^3}_a + \underbrace{3p^3 x^2 (1-x)}_b + \underbrace{3p^2 (1-p) x^2}_c. \quad (6)$$

Figure 14 displays the different situations which enter the above equation. The solutions are  $\frac{1}{2p^3} \left( \frac{3}{2}p^2 \pm \frac{1}{2}\sqrt{-8p^3 + 9p^4} \right)$  and 0. Since  $-8p^3 + 9p^4 \geq 0$  is needed to have a positive nonzero solution we get for the critical probability  $p_c = \frac{8}{9} \simeq 0.88889$ .

In a similar fashion one can derive a recursion equation for the generalized tree case. For that let  $T_R(2, 1)$  be the rooted generalized tree shown in Fig.15. To every vertex is attached an outgoing triangle, hence the degree of a vertex is 4 except the root which has degree 2. To settle the question about  $p_c$  for the original generalized tree it is enough to analyze the corresponding problem

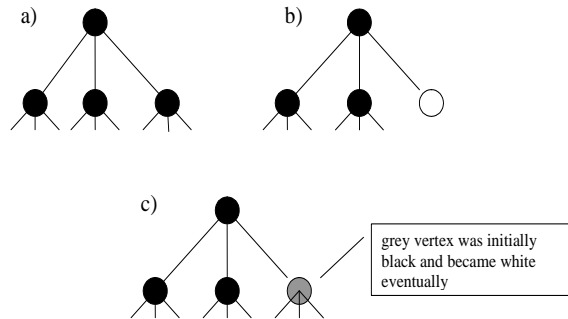


Figure 14: Different configurations in the neighborhood of the root vertex.. Black denotes vertices in an immune cluster and grey an initial black vertex which became white.

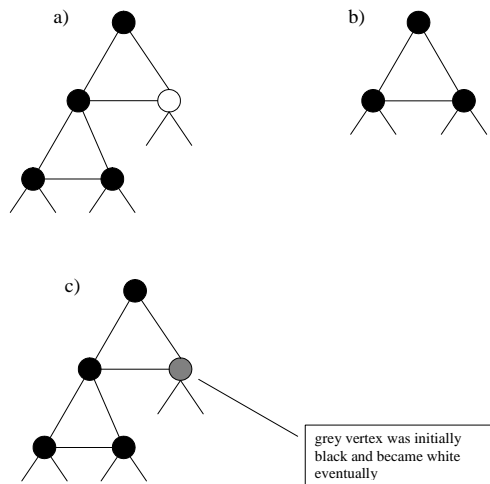


Figure 15: The local picture around the root vertex in  $T_R(2,1)$

for  $T_R(2, 1)$ . Again let  $x$  be the probability that the root vertex is in an immune cluster conditioned that the root is initially black. One gets the following recursion equation

$$x = \underbrace{p^2 x^2}_b + \underbrace{2p^4 x^2 (1-x)}_c + \underbrace{2p(1-p)p^2 x^2}_a \quad (7)$$

(see Fig.15). The solutions are  $\frac{1}{2p^4} \left( \frac{1}{2}p^2 + p^3 \pm \frac{1}{2}\sqrt{-7p^4 + 4p^5 + 4p^6} \right)$  and 0. Again since  $-7p^4 + 4p^5 + 4p^6 \geq 0$  is needed to get a positive nonzero solution we get for the critical probability  $p_c = \sqrt{2} - \frac{1}{2} \simeq 0.91421$ . That means the presence of clustering in this example lowers the critical initial density needed to infect the whole graph by almost a factor of  $\frac{3}{4}$ .

The study of the regular 4-tree generalizes easily to the case of regular  $n+1$ -trees ( $n > 2$ ). The recursion equation in this case is

$$x = p^n x^n + np^n x^{n-1} (1-x) + np^{n-1} (1-p) x^{n-1} . \quad (8)$$

A straightforward but lengthy computation gives for the critical probability

$$p_c = \frac{(n-1)^{2n-3}}{n^{n-1} (n-2)^{n-2}}; n > 2 . \quad (9)$$

In the special case of a 3-tree ( $n = 2$ ) one obtains  $p_c = \frac{1}{2}$ . For completeness we give without proof the formula for the computation of the critical probability in case of a rooted random tree with arbitrary outdegree distribution. Let  $g(z) = \sum_{i \geq 2} a_i z^i$  be the generating function for the outdegree; that is  $a_i$  is the probability that a random chosen vertex has outdegree  $i$  (and hence total degree  $i+1$ ). The critical probability  $p_c$  is given by the smallest  $p$  such that the equation

$$\frac{z}{p} = (1-z)g'(z) + g(z) \quad (10)$$

has a positive real solution.

A careful reader may have noticed that there is a big structural difference between the generalized tree in example 2 of section 3 and the generalized tree just discussed above. Namely the graph of the first example has the property, that any two vertices can be linked by a chain of triangle where neighbor triangles always have a common edge. The graphs in the examples of this section do not have this property since neighboring triangles have only

a common vertex. For threshold values  $\Delta > 2$  one has to consider chains of  $\Delta + 1$  cliques. We say that a graph is well  $k$ -linked if any pair of vertices can be linked by a chain of complete graphs of order  $k$  such that all neighboring  $k$ -cliques have a  $k - 1$ -clique in common. For well  $k$ -linked graphs the critical density  $b_c^0$  is zero (a finite number of initially infected vertices can already infect a positive fraction of the vertex set) for  $\alpha$ -processes with  $\Delta < k$  whereas for graphs which are not well linked one needs a positive critical density.

The above study on trees or generalized trees is insofar important as in most random graph models used for complex networks one has as a tree or generalized tree as the typical local structure around a random chosen vertex. Furthermore the dependence of the corruption dynamics on graph properties like edge density or degree distribution is in large parts of the parameter space entirely caused by the  $\alpha$ -process.

## 6 State and individual (mean field $\beta$ - and $\gamma$ - process)

In this section we want to have a closer look at the mean field dependence of the corruption process. To gain some insight in the possible type of behavior we start with some simple assumptions which will be refined later on. Again we will argue in a discrete time model but the transition to continuous time makes no problem and gives the same results. Let  $b_t$  the density of corrupt people at time  $t$ . We assume that the affinity for an individual to change its behavior from noncorrupt to corrupt increases proportional to the corruption prevalence. Furthermore to become really corruptly minded an individual has to overcome some fear which we put proportional to  $(1 - b_t)$ . Formally this reads as  $\Pr \{ \omega(x, t + 1) = 1 \mid \omega(x, t) = 0 \} = \beta b_t^2$  with  $\beta \in [0, 1]$ . Corrupt individuals can recover due to state and police effects (uncovering, fear etc.). Again it seems reasonable to assume that the probability to recover is proportional to  $1 - b_t$  since only the noncorrupt part of a society is willing to fight corruption. Formally we will assume that  $\Pr \{ \omega(x, t + 1) = 0 \mid \omega(x, t) = 1 \} = \gamma (1 - b_t)$  with  $\gamma \in [0, 1]$ . This gives

$$\begin{aligned} b_{t+1} &= (1 - b_t) \beta b_t^2 + b_t - b_t \gamma (1 - b_t) \\ &= b_t (1 - \gamma) + b_t^2 (\gamma + \beta) - b_t^3 \beta \end{aligned} \tag{11}$$

with the two obvious fixed points 0 and 1. For  $\beta \neq 0$  there is a third intermediate fixed point  $b^* := \frac{\gamma}{\beta}$ . An interesting phenomena happens for parameter pairs  $(\beta, \gamma)$  s.t.  $\gamma < \beta$  since under this conditions both fixed points at 0 and 1 are locally stable. Hence there are two basins of attraction- one for 0 and one for 1- with  $b^*$  as the boundary point. In other words, if the initial percentage of corruption is less  $b^*$  corruption stays under control whereas for an initial value larger  $b^*$  things run out of control and a corruption collapse takes place. Of course this mean field part of the model is still very simplistic and one should not expect any quantitative fit with empirical data. But the qualitative statement seems to be quite stable with respect to modifications. For instance there are good reasons to believe that neither the mean field infection nor the mean field recover process are linear in  $b_t$ .

We want to end this section with a small modification of the mean field "Ansatz" where we include social weights. This is a natural and meanwhile very common approach in network dynamics and can easily be adopted to the corruption model. In the above argumentation on the attraction of becoming corrupt it is plausible to assume that corrupt individuals with high social influence have a stronger influence on the mean field probability to get corrupt than individuals with low social importance. A similar argument holds for the recover probability. As a simple measure for social strength we use the degree of the vertices since high degree vertices are more likely to play a dominant social role than low degree vertices. Formally we introduce the weighted density  $b_t^w$  at time  $t$  as

$$b_t^w := \frac{\sum_k I_t^{(k)} d_k}{\sum_k (d_k)^2} \quad (12)$$

where  $d_k$  is the number of vertices with degree  $k$  and  $I_t^{(k)}$  the number of corrupt (state 1) vertices with degree  $k$  at time  $t$ . The mean field equation for group  $k$  is now given by

$$I_{t+1}^{(k)} = \beta (b_t^w)^2 (d_k - I_t^{(k)}) + I_t^{(k)} - \gamma (1 - b_t^w) I_t^{(k)} \quad (13)$$

. Multiplying the last equation by  $\frac{d_k}{\sum_k (d_k)^2}$  and summing over  $k$  gives

$$b_{t+1}^w = (1 - b_t^w) \beta (b_t^w)^2 + b_t^w - b_t^w \gamma (1 - b_t^w) \quad (14)$$

which is the same as equation (11). Therefore the introduction of social weights does not add anything new to the dynamical picture. There is of course a difference in the interpretation since a small real initial prevalence of corruption can give rise to a high initial value of  $b_0^w$  as soon as the corruption is concentrated at the high degree vertices. Here also a difference between scale free networks and classical random networks is seen since in the scale free case high degree vertices (hubs) are much more frequent than in the classical case.

## 7 Interaction between the mean field process and the local threshold dynamics ( $\beta + \gamma$ versus $\alpha$ )

In this paragraph we will investigate some aspects of the interplay between the mean field process described in the previous section and the local, threshold dependent, corruption propagation. For  $\alpha > \gamma$  there is a core infected component generated via the  $\alpha$ - process. To gain some insight how such a core infected part of the population changes the mean field dynamics we will assume that a certain fraction, say  $a$ , of the population is permanently infected and resistant to the  $\gamma$ -deletion process. Denoting by  $q_t = b_t - a$  the density in the noncore part of the population (the normalization here is still with respect to the total population size) we get the following mean field dynamics:

$$\begin{aligned} q_{t+1} &= (1 - a - q_t) \beta (q_t + a)^2 + q_t - q_t \gamma (1 - a - q_t) \\ &= a^2 \beta - a^3 \beta + q_t (2a\beta - \gamma + a\gamma - 3a^2 \beta + 1) + \\ &\quad + q_t^2 (\beta + \gamma - 3a\beta) - \beta q_t^3 \end{aligned} \tag{15}$$

. Since the state where all individuals are infected is stationary we get the following set of fixed points:

$$\left\{ -a + 1, \frac{1}{\beta} \left( \frac{1}{2} \gamma - a\beta - \frac{1}{2} \sqrt{-4a\beta\gamma + \gamma^2} \right), \frac{1}{\beta} \left( \frac{1}{2} \gamma - a\beta + \frac{1}{2} \sqrt{-4a\beta\gamma + \gamma^2} \right) \right\}$$

. For  $-4a\beta\gamma + \gamma^2 < 0$  there are no real fixed points except  $q^* = -a + 1$  which becomes globally stable under this condition. Since we have a polynomial of degree 3 we get  $\frac{1}{\beta} \left( \frac{1}{2} \gamma - a\beta + \frac{1}{2} \sqrt{-4a\beta\gamma + \gamma^2} \right) < 1$  as the condition for

the fixed point at  $1 - a$  to be locally stable. Furthermore in this case also the fixed point at  $\frac{1}{\beta} \left( \frac{1}{2}\gamma - a\beta - \frac{1}{2}\sqrt{-4a\beta\gamma + \gamma^2} \right)$  becomes a local attractor. This is for instance the case when  $a$  becomes very small and  $\beta > \gamma$  - being back essentially in the situation of the previous section. In case when  $\frac{1}{\beta} \left( \frac{1}{2}\gamma - a\beta + \frac{1}{2}\sqrt{-4a\beta\gamma + \gamma^2} \right) > 1$  it is easy to show that the fixed point at  $\frac{1}{\beta} \left( \frac{1}{2}\gamma - a\beta - \frac{1}{2}\sqrt{-4a\beta\gamma + \gamma^2} \right)$  becomes a global attractor (to see this just note that the derivative at  $q_t = 0$  is always positive for the relevant parameter intervals). The above considerations show that the possible dynamical evolution scenarios are the same for  $a = 0$  and  $a \neq 0$ . But there is a very strong influence of  $a$  on the parameter regimes of  $\beta$  and  $\gamma$  for which one has a corruption collapse. Whereas in case  $a = 0$  one is always in the basin of attraction of zero for  $b_0$  sufficiently small and  $\gamma \neq 0$  (in other words  $b = 1$  is never a global attractor) one can now have the phenomenon that only the complete saturation with corruption is stable ( $q = 1 - a$ ). As an example lets look at the case where  $\beta = 2\gamma$ . For  $a = 0$  there is a fixed point at  $b^* = 0.5$  and hence for an initial infection density  $b_0 < 0.5$  the pure mean field dynamics converges to zero. In the case  $a \neq 0$  one has for  $a > 1/8$  only the stable fixed point  $b^* = a + q^* = 1$ . At  $a = 1/8$  there is a phase transition since a new indifferent (slope 1) fixed point at  $b^* = 1/4$  emerges. For  $a < 1/8$  this fixed point bifurcates into two fixed points where the first one at  $b^* = \frac{1}{4} - \frac{1}{4}\sqrt{1 - 8a}$  becomes locally stable with a basin of attraction given by  $b_0 < \frac{1}{4} + \frac{1}{4}\sqrt{1 - 8a}$ .

We close this section by presenting a numerical result showing the different contributions to the overall infection (end-prevalence) of the local and mean field processes as a function of the edge density in the random graph space  $\mathcal{G}(N, M)$ . Fig.16 gives the accumulated number of state changes (divided by  $N$ ) caused by the  $\alpha, \beta, \gamma$  and  $\varepsilon$ - process at initial density values slightly above the critical one. Up to an edge density of 2 (corresponding to a mean degree of 4) the  $\beta$ - process gives the major contribution to the end prevalence in the overcritical situation. Parallel to the increase in the edge density increases the contribution of the  $\alpha$ - and  $\varepsilon$ - process (in the intermediate phase of density between 2 and 3 dominated by the  $\alpha$ - process) till a sharp peak at edge density 4.5 where the  $\varepsilon$ - process outperforms all the others (at the same time the critical initial corruption density  $b_0^c$  drops down and becomes almost zero). The peak is easy to understand since for the chosen parameters we have at an edge density of 4 an equality between

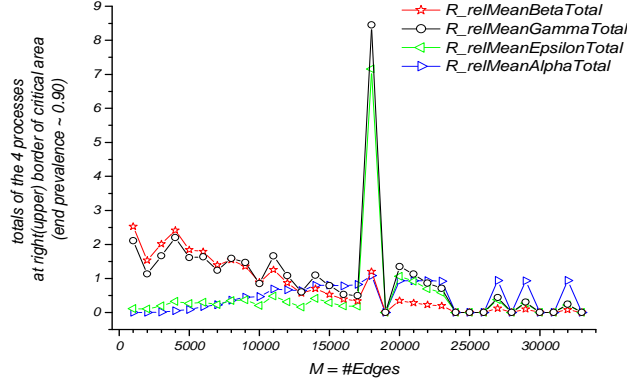


Figure 16: The total number of state changes splitted according to the  $\alpha$ ,  $\beta$ ,  $\gamma$  and  $\varepsilon$ - process for the following parameter values in a  $\mathcal{G}(N, M)$  graph:  $N = 4000$ ;  $\alpha = 0.35$ ;  $\beta = 0.08$ ;  $\gamma = 0.04$ ;  $\varepsilon = 0.005$ ;  $\Delta = 5$ .

the recover rate  $\gamma$  and the expected number of new corruptions caused by a single corrupt vertex via the  $\varepsilon$ - process (which is  $\mathbb{E}(d(x)) \cdot \varepsilon$ ). In terms of classical epidemic processes this corresponds to the case of reproduction number  $R_0 = 1$ . Above this value single initial corrupt vertex is already enough to cause in conjunction with the mean field process a total infection of the network.

## 8 Single run simulation results

In this section we want to present some simulation results of the corruption process taking place on some medium size complex networks. Small graph sizes are interesting as they are typical for communities in highly social structured populations. As a simple to generate random graph space with high clustering and power law degree distribution we have chosen so-called intersection graphs. Intersection graphs can easily be defined as follows. First one forms random sets from a finite base set of  $N$  elements (random means in this context that the set elements are chosen uniform i.i.d. from the base set). These sets constitute the vertices of a random graph. Edges will be defined via the set intersection property, namely there is an edge between  $i$

<b>graph characteristic</b>	<b>FP2 (1987-1991)</b>	<b>FP3 (1990-1994)</b>
# vertices	4879	7710
# edges	57633	93852
mean degree	23.624	24.346
maximal degree	844	1014
# vertices wiht degree $> 5$	3865	6051
size of largest component	4775	7356
mean # triangles per vertex	256.89	418.09
exponent of degree distribution	2.1	2.4

Table 2: Properties of the real networks FP2 and FP3

and  $j$  if the associated sets  $A_i$  and  $A_j$  have nonempty intersection. The size (cardinality)  $|A|$  of a set  $A$  is itself a random variable drawn i.i.d. from a pre-given probability distribution  $\varphi(k)$ . To get interesting graph spaces one furthermore requires  $N < \sum |A_i| < const \cdot N$ . For theoretical results about the structure of random intersection graphs see [7][12][11]. It is worth noting that intersection graphs have a high clustering by definition (if an element is contained in say  $k$  sets simultaneously this  $k$  sets form a complete subgraph). Most simulations were done for the case when  $\varphi$  is an asymptotic power law distribution with exponent 3 or when  $\varphi$  is singular (all sets have the same size). Random intersection graphs have a multiplicative degree correlation and therefore the critical threshold should be very low for exponents less than 3 be the arguments from section 5. Above that value the form of the degree distribution has only little influence on the corruption propagation.

Besides random intersection graphs generated according to some degree specifications we used also a collection of real collaboration graphs. These graphs come from a database about research and development projects funded by the European Community (FP2-3). It's vertices are organizations involved in European research projects. Two organizations are linked if they have a joint project (see table II for the main graph characteristics). In total the data base contains about 8000 projects and 13000 participating organizations. In essence the network shows all the main characteristics that are known from other complex network structures like scale free degree distribution (with exponent between 2 and 3), small diameter and high clustering and vertex correlation. The initial fraction of infected individuals was either distributed at random over the vertex set or clumped together in a sufficiently large ball

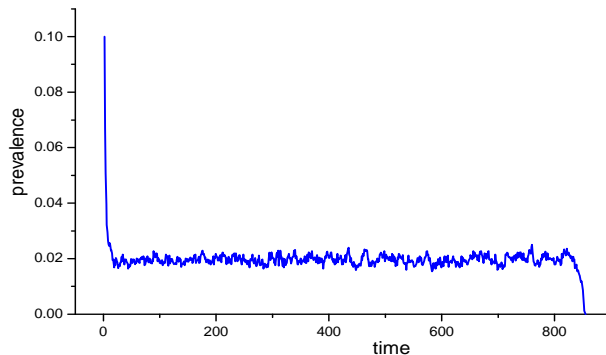


Figure 17: Low, semistable prevalence in a real collaboration network (FP2),  $\Delta=30$   $\varepsilon=0$ ,  $\alpha=0.99$   $\beta=0.09$   $\gamma=0.545$   $b_0=0.1$   $N=4879$

with a random chosen vertex as center.

In the following we want to give a small sample of simulations on the just mentioned graphs and try to discuss its main features. Fig.17 displays the prevalence of corruption on the real network FP2. The absolute threshold value  $\Delta = 30$  is very high and does not allow for a big outbreak of corruption. But there is a metastable small community of individuals, highly linked and almost resistant to the  $\gamma$ -process. It took more than 800 complete updates till this structure broke down.

The next figure 18 presents a similar situation on an almost twice as large real graph (FP3). In contrast to the previous case we have a much smaller  $\alpha$ -value and an only slightly reduced threshold  $\Delta$ . The network FP3 is extremely high clustered (mean degree = 48.6, mean triangle number = 418 and a total of 7710 nodes and 187704 edges) and stays metastable with a very small corruption cluster for about 200 updates till it jumps by a factor 10 to another metastable state. Fig.19 gives a more detailed view of the accumulated contributions by the different processes for a time interval around the jump in prevalence. In the initial phase the  $\varepsilon$ -process was dominating the  $\beta$ -process and vice versa in the second phase. The next pictures show a situation where after an initial phase of slow growth a corruption collapse happened. It seems that the absolute threshold value  $\Delta = 20$  is well below the critical value where the system can still stabilize.

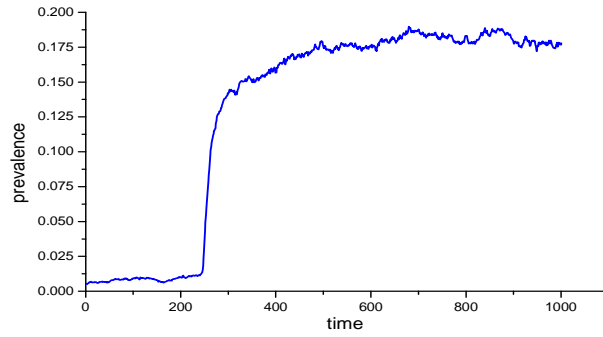


Figure 18: switch from a very low prevalence semi stable state to a low prevalence state (FP3),  $\Delta=25$ ,  $\varepsilon=0.001$ ,  $\alpha=0.2$ ,  $\beta=0.04$ ,  $\gamma=0.03$ ,  $b_0=0.005$ ,  $N=7710$

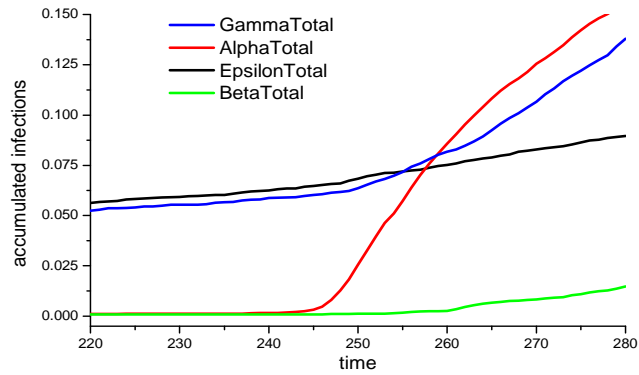


Figure 19: The contribution of the different infection paths for a segment of the prevalence curve in Fig. 18

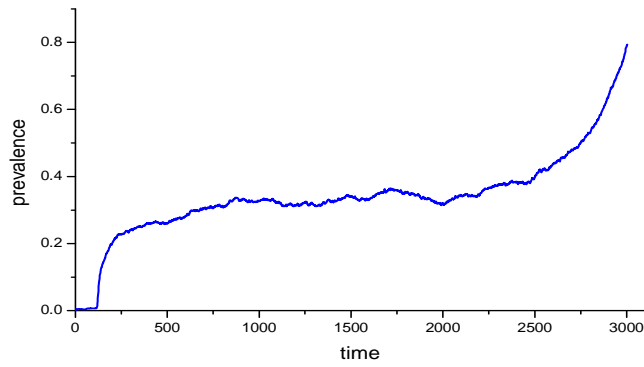


Figure 20: Slow increase of prevalence till collapse (FP3),  $\Delta=20$   $\varepsilon=0.001$   
 $\alpha=0.2$   $\beta=0.04$   $\gamma=0.03$   $b_0=0.005$

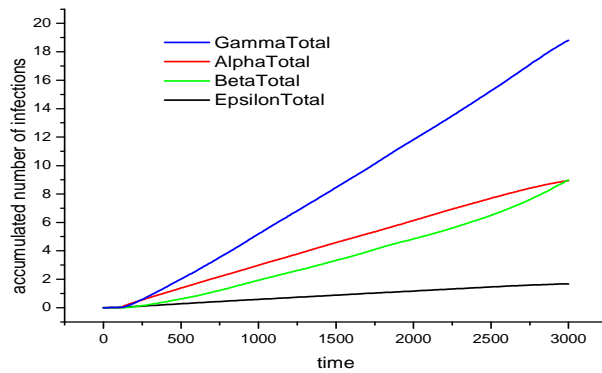


Figure 21: Accumulated infection processes for the situation in Fig.20.

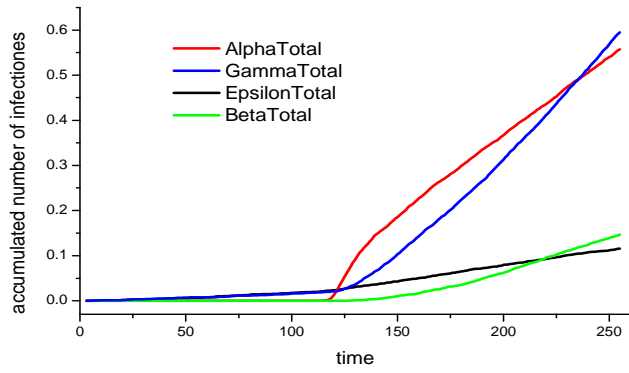


Figure 22: details for the initial phase from fig.20.

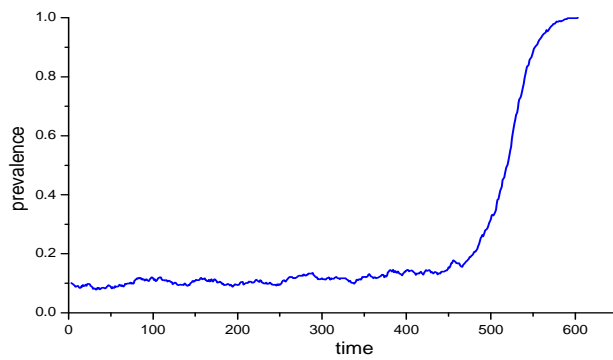


Figure 23:  $\Delta=8$   $\varepsilon=0.005$   $\alpha=0.1$   $\beta=0.09$   $\gamma=0.045$   $b_0=0.1$   $N=952$

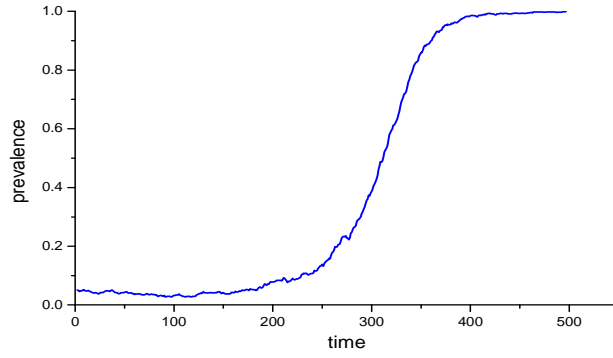


Figure 24: Slow corruption collapses in an artificial net  $\Delta=6$   $\varepsilon=0.005$   $\alpha=0.1$   
 $\beta=0.06$   $\gamma=0.05$   $b_0=0.05$   $N=972$

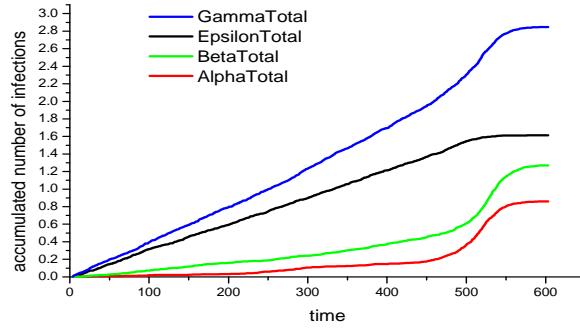


Figure 25: Process splitting for the situation in Fig.23

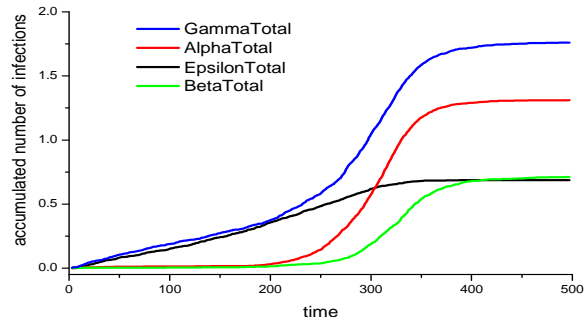


Figure 26: Process splitting for the situation from Fig.24

It is surprising that the system semi-stabilizes after an initial rapid increase in the prevalence for a rather long time (Fig.20). To a certain extent the results can be explained along the argumentation in section 7. In Fig.22 the accumulated infection processes for the initial phase are shown. Here the  $\varepsilon$ - process, although undercritical, causes a redistribution of infection till a clustered configuration is reached such that the  $\alpha$ - process can start. Then the system stays in almost complete balance till the  $\beta$ - process (which is slow in all our examples) wins (Fig.21). Note the difference to Fig.19, where the  $\beta$ - process never really contributes to the infection. Finally we show two simulations for a sample of a random set graph model with about 1000 vertices (Fig.23 and Fig.24). Although both prevalence curves look similar there is a clear difference in the process fine-structure (Fig.25 and Fig.26). In the first instance the  $\varepsilon$ - and  $\beta$ - process are causing the collapse whereas in the second case the  $\alpha$ - process in conjunction with the  $\varepsilon$ - process is the main booster.

The few examples of single simulation runs given in this section show already, that there are many different routes to obtain high prevalence in corruption typically interrupted by long phases of metastability. Similar to other complex systems with hidden phase transitions (e.g. the climate) there can be an unnoticed small accumulation of infection till a critical density- a point of no return- of corruption is reached from which on an almost complete saturation of the society (or a corresponding subsystem) by corruption becomes the normality.

## 9 Epidemic control

One of the basic question in classical epidemics as well as in corruption dynamics is: what can be done to slow down the "infection" propagation or prevalence. Knowing the different phase transitions and their dependency on structure properties and social parameters is of great help in designing proper prevention scenarios. In the following we will try to relate some of the findings from our model to what is considered by practitioners as useful in corruption reduction. First we would like to emphasize again that the present model deals in a rather abstract way with the propagation of mental willingness to be corrupt and not so much with realized corruption which always requires a specific environment and additional structural assumptions. Hence concerning corruption control, we only will be able to support certain prevention scenarios in the sense, that they go into the right direction and that there effect is strong or weak but without being able to make quantitative statements.

The model presented in this paper contains, besides structural parameters for the underlying network, 5 relevant parameters:  $\alpha$ - characterizing the strength of the local threshold process,  $\beta$ - characterizing the strength of the mean field attraction on becoming corrupt,  $\gamma$ - the strength of the "society strikes back" term,  $\varepsilon$ - the strength of the classical epidemic process (assumed to be very small) and  $\Delta$ - the height of the local threshold. Three of the parameters-  $\alpha$ ,  $\beta$  and  $\varepsilon$ - are positively correlated to the spread of corruption whereas 2 parameters-  $\Delta$  and  $\gamma$ - are negatively correlated. As is well known from classical epidemic control for infectious diseases it is very hard if not impossible to change basic social parameters in a short time. This can only be achieved in a long running educational process. Therefore not much can be done in avoiding high clustering in certain relevant areas of the society in order to prevent the emergence of highly connected corruption nets.

As the name already indicates, Transparency International favours as an effective tool to decrease corruption especially the increase of transparency in all forms of administrative decision making as well as transparency in financial affairs of socially exposed persons, institutions and companies. The effect of an increase of transparency translates into our model as an increase of the value of  $\Delta$  and a decrease of the values of  $\beta$ ,  $\alpha$  and  $\varepsilon$ . Strengthening of justice, police and similar instruments to fight and uncover corruption has again the effect of lowering  $\beta$  (via increase of fear) but may also increase the value of  $\gamma$  (uncovering rate). Since an increase of  $\gamma$  above the value of  $\beta$  and

$\alpha$  would perhaps require a total police state, it is illusionary to overcome corruption just by means of law, justice and police. Besides necessary long term educational efforts in school and public to strengthen the moral resistance against corruption (increase of  $\Delta$  and decrease of  $\alpha$ ) it seems a good strategy to make administrative and political decision hierarchies as independent and decentralized as possible to avoid high clustering.

We would like to end these short remarks by a few comments on the role of hubs - the very high degree vertices typically present in scale free graphs - in corruption dynamics. While a priori not especially well suited to transmit corruption via the  $\alpha$ - process due to the local tree like structure around the hubs (compared with low degree vertices) they nevertheless are more often exposed to corruption and have therefore a higher probability to get corrupt. If the hub density is sufficiently high (as is the case for scale-free degree distributions with exponent  $\lambda < 3$ ) and the degree correlation is stronger than additive many vertices are linked to the hubs via social dependencies and in turn also can get corrupt. Furthermore they may play a fatal role in increasing the weighted corruption density relevant for the mean field process as was explained at the end of section 7. The described situation is probably typical for strongly hierarchically organized countries or regional substructures e.g. systems with a dictatorial or monarchical tendency. In such societies a high prevalence of corruption seems almost unavoidable since the threshold  $b_0^c$  is close to zero. For democratic societies it seems therefore wise, to watch the behavior of hubs- whatever their social interpretation might be- more intensively than the "normal" part of the society.

## 10 Summary and perspectives

In this article we have presented a first study of the spread of corruption on scale free and highly clustered networks. One of the main observations so far is the strong dependence of the asymptotic dynamics on the initial number of corrupt individuals. This holds as well for the mean field process as for the local dynamics. Second there is a fatal resonance effect between global and local dynamics lowering dramatically the critical density of initial infection. As expected there is a positive correlation between clustering and spread of corruption respectively the critical initial density. Scale-freeness seems to play an important role for the corruption process for distributions with small exponent ( $\lambda < 3$ ) and multiplicative degree correlation due to

the high prevalence of infected hubs and the strong linkage of medium and low degree vertices to them. For higher exponents the dynamics is rather insensitive to the degree distribution. The strength of the degree correlation (from weak - additive till strong - multiplicative or even higher powers) in networks of social acquaintances seems to be related to the political and institutional structure of a society which favours liberal organization forms as being less vulnerable to corruption.

There is a whole bunch of natural continuations or generalizations which have to be investigated next. Clearly a deeper understanding of the pure  $\alpha$ -process and its phase transitions is necessary. The mathematical problem is already highly nontrivial on trees. The following short list gives a selection of natural generalizations and refinements:

- quenched disorder in all parameters
- inclusion of geographical or regional structure into the network
- inclusion of administrative or political substructures in which corruption typically will be realized
- evolving networks
- interaction between the corruption process and the network structure
- more heterogeneity in the social networks e.g. by incorporating family like structures or social profiles
- weighted networks
- refined transition rules e.g. asymmetry between infecting and getting infected
- different kinds and strength of corruption and their interplay
- economic impacts in a virtual population.

Besides the specific context of corruption dynamics there is a multitude of topics where the model presented in this paper could easily be adopted to. This includes so different themes as political opinion formation, social disorder processes, strategies for advertisement, doping usage, the spread of prejudices, migration dynamics, global terrorist networks and innovation

processes. In all these examples one has a local and global dynamics very similar to the one described here. Of course there are differences. For instance in many mind formation problems the state space of individuals is rather complex and the local dynamics allows for many transitions not just 0-1 as in the corruption model. Furthermore aging phenomena and limits of resources could be included. But besides this addition of structure and complexity and the various interpretations there remains a good part of the findings of this work to be true. There will be phase transitions in the initial density of certain properties and there can be resonance effects between the nonlinear global and local dynamics - both making the prediction of future difficult and challenging.

**Acknowledgements** We would like to thank for the support of the Volkswagen Foundation, the DFG-Research Group 399 "Spectral Analysis, Asymptotic Distributions and Stochastic Dynamics" and the Austrian Research Center Seibersdorf for providing us with the data set of EU-funded research projects. P. Martin especially thanks Klaus Geppert, Detlef Leenen, Christian Pestalozza and Albrecht Randelzhofer for stimulating discussions.

## References

- [1] R. Albert, A.-L. Barabasi: *Statistical Mechanics of Complex Networks*, Reviews of Modern Physics, **74**, 47 (2002), arXiv:cond-mat/0106096
- [2] J. Andvig, O.-H. Fjeldstad, I. Amundsen, T. Sissener, T. Søreide: *Research on Corruption, a policy motivated survey*, Norwegian Agency for Development Co-operation, NORAD, Final report 2000
- [3] B. Bannenberg: *Korruption in Deutschland und ihre strafrechtliche Kontrolle*, (2002), www.im.nrw.de
- [4] Ph. Blanchard, T. Krueger: *The "Cameo principle" and the origin of Scale-free graphs in social networks*, Journal of Statistical Physics, **114**, 5-6 (2004), arXiv: cond-mat/0302611
- [5] Ph. Blanchard, C. Chang, T. Krueger: *Epidemic thresholds on scale-free graphs: the interplay between exponent and preferential choice*, Annales Henri Poincaré vol. 4, suppl.2, (2003), arXiv: cond-mat/0207319

- [6] Ph. Blanchard, T. Krueger, A. Ruschhaupt: *Small world graphs by iteration of local edge formation*, to appear in Phys.Rev.E (2005), arXiv: cond-mat/0304563
- [7] Ph. Blanchard, T. Krueger: *Random scale free intersection graphs and related bipartite structures*, in preparation
- [8] Ph. Blanchard, S. Fortunato, T. Krueger: *Do extremists impose the structure of social networks?*, arXiv:cond-mat/0407434 (2004), to appear in Phys. Rev. E
- [9] P. Dodds, D. Watts: *Universal behavior in a generalized model of contagion*, arXiv:cond-mat/0403699 (2004)
- [10] Ch. Ellis, J. Fender: *Corruption and Transparency in a Growth Model*, preliminary draft (2003)
- [11] J. Fill, E. Scheinerman, K. Singer-Cohen: *Random intersection graphs when  $m=(n)$ : An equivalence theorem relating the evolution of the  $G(n, m, p)$  and  $G(n, p)$  models*, Random Structures and Algorithms **16**, 2 (2000)
- [12] M. Karonski, E. Scheinerman, K. Singer-Cohen: *On random intersection graphs: the subgraph problem*, Combinatorics, Probability and Computing **8** (1999)
- [13] P. Newman: *The spread of epidemic disease on networks*, Phys. Rev. E **66**, 016128 (2002)
- [14] P. Newman, J. Park: *Why social networks are different from other types of networks*, Phys. Rev. E **68**, 036122 (2003)
- [15] R. Pastor-Satorras, A. Vespignani: *Epidemic Spreading in Scale-Free Networks*, Phys.Rev.Lett.**86**, 3200 (2001)
- [16] S. Shi, T. Temzelides: *A Model of Bureaucracy and Corruption*, International Economic Review **45**, 3 (2004)
- [17] T. Steinrücken: *Illegale Transaktionen und staatliches Handeln*, Deutscher Universitätsverlag 2003

- [18] Transparency International: *CPI 2004*, <http://www.transparency.org/cpi/2004/cpi2004.en.html>
- [19] F. Wirl : *Socio-economic typologies of bureaucratic corruption and implications*, *Evolutionary Economics*, **8** (1998)